SI APPENDIX

Pedrolli et al.

SI Methods

Bacterial strains, plasmids and growth conditions. *E. coli* TOP 10 was used as a host for gene cloning experiments. *E. coli* BL21(DE3) was used as a host for the synthesis of different variations of recombinant RibR. *E. coli* CpXFMN is a recombinant strain which constitutively produces the riboflavin importer RibM from *Corynebacterium ammoniagenes* (1). *B. subtilis* 168 (2) is a wild-type strain. The *ribR* deletion *B. subtilis* strain (*ribR::aph3*) was constructed as described (3). The *B. subtilis* strain overexpressing *ribR* was generated employing pHT01 (Mobitech, Göttingen, Germany). Construction of a recombinant *B. subtilis* strain which produces RibR-TAP-tag is described in the supplement. Details with regard to the construction of plasmids also can be found in the supplement. If not otherwise stated *E. coli* was aerobically cultivated at 37°C on Lysogeny Broth (LB) or on M9 minimal medium (supplemented with 0.1% casamino acids) containing antibiotics and other additives (4). *B. subtilis* was aerobically grown at 37°C in LB or in a minimal medium (5). The sulphur source varied in the different experiments as stated: 5 mM taurine/1 mM methionine or 4 mM $MgSO_4$.

Construction of plasmids. The plasmid pRibR-TAP-tag was constructed by ligating a *Kpn*I/*Pst*I digested PCR product (generated using oligonucleotides 1 and 2, Table S2) representing the 3'-part of *Bacillus subtilis ribR* to *Kpn*I/*Pst*I digested pSG1164-TAP (6). The plasmid pPrib-luc was constructed as follows. Oligonucleotides 3 and 4 (Table S2) generated a linker which was used to replace the T7 promoter of pT7luc^{mod} (7) by the promoter Prib of *Escherichia coli*, which naturally is responsible for expression of *E. coli ribB* coding for the riboflavin biosynthetic enzyme 3,4-dihydroxy-2-butanone-4-phosphate synthase (Mendoza-Vargas et al., 2009). The oligonucleotides (10 µM each) were annealed in TE (10 mM Tris-HCl pH 8.0, 1 mM EDTA). The mixture was heated to 98°C for 5 min and slowly cooled to

20°C. The resulting dsDNA linker contained sticky ends allowing ligation to *Pvu*II/*Hin*dIII digested pT7luc^{mod}. The plasmids pPrib-RibDG-RFN-luc and pPrib-RibU-RFN-luc were generated as follows. The DNA fragments coding for the two different *B. subtilis* FMN riboswitches (*ribDG* and *ribU*) were produced by PCR using the modifying oligonucleotides 5/6 and 7/8 (Table S2) which introduced restriction sites (*Bam*HI/*Hin*dIII) for cloning. The resulting DNA-fragments were ligated to *Bam*HI/*Hin*dIII digested pPrib-luc. The ligation products were used to transform *E. coli* Top10. The newly constructed plasmids were isolated from the corresponding recombinant *E. coli* strains using the GeneJET™ Plasmid Miniprep Kit (Fermentas, Heidelberg, Germany). The isolated plasmids were again purified using the same kit and eluted from the anion exchange columns with nuclease-free water to serve as templates for *in vitro* transcription/translation reactions. In addition, the plasmid constructs were used to transform *E. coli* CpXFMN for coexpression experiments. The derivatives of pPrib-RibDG-RFN-luc, pPrib-RibDG-RFN^{MutOn}-luc and pPrib-RibDG-RFN^{MutOff}-luc, were generated using the QuikChange II XL Site-directed Mutagenesis Kit (Agilent, Waldbronn, Germany). Oligonucleotides 9/10 (Table S2) were used to replace nucleotides GGG by CCC at positions 23, 24, 25 of the *ribDG* FMN riboswitch aptamer domain (ON mutant). Oligonucleotides 11/12 (Table S2) were used to replace nucleotides GGG by CCC at positions 18, 19, 20 of the *ribDG* FMN riboswitch aptamer domain (OFF mutant). The resulting plasmids were used to transform *E. coli* Top10. The newly constructed plasmids were isolated from the corresponding recombinant *E. coli* strains using the GeneJET™ Plasmid Miniprep Kit (see above). The plasmid pPrib-RibE-RFN-luc was generated by ligating a *Bam*HI/*Hin*dIII-fragment containing the *ribE* FMN riboswitch from *Streptomyces davawensis* (7) to *Bam*HI/*Hin*dIII digested pPrib-luc. The plasmids pT7-RFNapt-RibDG and pT7-RFNapt-RibU were used as templates for *in vitro* transcription reactions to generate full-length FMN riboswitch RNA molecules (gel shift assays). The plasmids were sequentially assembled employing three separately produced DNA molecules. Oligonucleotides 13 and 14

(Table S2) were used to create a linker (*Eco*RI and *Xho*I compatible) to introduce a T7 promoter into the constructs. DNA fragments coding for the two different FMN riboswitch aptamer domains (*ribDG* and *ribU*) were generated by PCR using the modifying oligonucleotides 15/16 and 17/18 (Table S2) which introduced restriction sites (*Xho*I/*Hin*dIII) for cloning. *Eco*RI and *Hin*dIII digested pSP64 (Promega, Mannheim, Germany) was used as a backbone. The linker, the aptamer domains and digested pSP64 were ligated to each other and the resulting product was used to transform *E. coli* Top10. The following plasmids were used in the coexpression experiments. The inserts of pET28a-ribRfull, pET28a-ribRC-terminus and pET28a-ribRN-terminus were generated by PCR employing the modifying oligonucleotides 19 and 20 (encoding full length RibR), 21 and 20 (encoding the C-terminal amino acids 1-123 of RibR), 19 and 22 (encoding the N-terminal amino acids 124-230 of RibR) which introduced restriction sites (*Nde*I/*Xho*I) for cloning. The PCR products were treated with *Nde*I/*Xho*I and ligated to *Nde*I/*Xho*I digested pET28a (Novagen, Darmstadt, Germany). The resulting constructs were used to transform *E. coli* BL21. The plasmids pMAL-ribRfull, pMAL-ribRC-terminus and pMAL-ribRN-terminus were used for overproduction of the different maltose binding protein (MBP) fusions of RibR in *E. coli*. pET28a-ribRfull, pET28a-ribRC-terminus and pET28a-ribRN-terminus (see above) were treated with *Nde*I and *Xho*I. The resulting fragments were ligated to *Nde*I/*Sal*I digested pMAL-c5X (New England BioLabs, Frankfurt, Germany). The ligation products were used to transform *E. coli* ER2523 (New England BioLabs). The plasmid pHT01ribR was constructed as follows. A DNA fragment coding for RibR was generated by PCR using the modifying oligonucleotides 23 and 24 (Table S2) which introduced restriction sites (*Xba*I/*Sma*I) for cloning. The PCR product was ligated to *Xba*I/*Sma*I digested pHT01 (MoBiTec, Göttingen, Germany). The resulting construct was used to transform *B. subtilis* Marburg 168 (wild-type).

Construction of a recombinant *B. subtilis* strain which produces RibR-TAP-tag. pRibR-TAP-tag was used to transform wild-type *B. subtilis*. Single crossover recombination

produced strains which contained the recombinant *ribR* version (producing "TAP-tagged" RibR) directly downstream of *cmoJ*.

Metabolome analysis. The mass spectrometric analysis was performed on a platform consisting of a Hitachi L-7100 liquid chromatography pump coupled to a Gerstel MPS2 autosampler and an Agilent 6550 IonFunnel QTOF (Agilent, Santa Clara, CA) operated with published settings in negative ionization mode (8) using automated isocratic flow-injection without prior chromatographic separation. The flow rate was 150 µL/min of mobile phase consisting of isopropanol/water (60:40, v/v) buffered with 5 mM ammonium fluoride at pH 9. For online mass axis correction, 2-propanol (in the mobile phase), taurocholic acid, and hexakis (1*H*, 1*H*, 3*H*tetrafluoropropoxy)phosphazine (Agilent Technologies) were added to the mobile phase. All samples were measured in technical duplicates. Mass spectra were recorded in profile mode from *m/z* 50 to 1,000 with a frequency of 1.4 spectra/s for 0.48 min using the highest resolving power (4 GHz HiRes). Source temperature was set to 325°C, with 5 L/min drying gas and a nebulizer pressure of 30 psig. Spectral processing (profile alignment, peak detection, centroiding, merging) was performed as published previously (8). All steps of data processing and analysis were performed with Matlab R2014a (The Mathworks, Natick) using functions embedded in the Bioinformatics, Statistics, Database, and Parallel Computing toolboxes. All ions were annotated within 0.001 Da deviation from their theoretical mass. Cells were harvested by centrifugation (5 min, 0 °C, 4,500 rpm) and immediately frozen in liquid nitrogen. Frozen cells were suspended in 2 mL of acetonitrile:water (60:40; v/v) preheated to 80°C and the mixture was further incubated at 80°C for 3 min. Subsequently, the mixture was placed on ice for 2 min. Debris were removed by centrifugation (5 min, 4 °C, 15,000 rpm). The supernatant was collected and dried under vacuum at 30°C. Samples were suspended in 100 µL ultrapure water and analyzed in technical duplicates by flow-injection time-of-flight mass spectrometry (8) with an Agilent 6550 QToF instrument

Western blot analysis of *B. subtilis* proteins. *B. subtilis* cells were harvested and washed three times using 50 mM Tris-HCl (pH 8.0). Cells were suspended in 1 mL freshly prepared and prewarmed (37°C) TMS buffer (50 mM Tris-HCl pH 8.0, 16 mM $MgCl_2$, 33% m/v sucrose). Subsequently, lysozyme (300 µg mL^{-1}) and phenylmethylsulfonylfluoride (1 mM) were added and the mixture was incubated for 30 min at 37°C. The resulting protoplasts were cooled to 4°C, harvested by centrifugation (1 min, 7,500 x g), resuspended in 1 mL lysis buffer (50 mM Tris-HCl pH 8.0, 5 mM $MgSO_4$) containing 1 mM phenylmethylsulfonylfluoride and sonified on ice. Membranes were collected by centrifugation (30 min, 100,000 x g), washed once with 50 mM Tris-HCl pH 8.0 and suspended in 50 µl 50 mM Tris-HCl pH 8.0. The samples were analyzed by SDS-PAGE on 4-20% gradient polyacrylamide gels using 10-20 µg of protein per lane. After transfer to nitrocellulose membranes proteins were immunologically detected. Monoclonal mouse anti-penta-His primary antibodies/goat anti-mouse IgG alkaline phosphatase(AP)-coupled secondary antibodies (Novagen, Darmstadt, Germany) were used for His_6-tag detection. AP was detected with the "AP Detection Reagent Kit" (Novagen) using 3-bromo-4-chloro-5-indolyl phosphate and nitro blue tetrazolium chloride. Monoclonal mouse anti-TAP α-protein antibodies/goat anti-mouse IgG Horseradish peroxidase (HRP)-coupled secondary antibodies were used for TAP-tag detection. Horseradish peroxidase activity was measured with HRP substrate (CN/DAB Substrate Kit, Thermo Scientific). Polyclonal rabbit anti-riboflavin synthase (RibE) primary antibodies and IgG alkaline phosphatase(AP)-coupled secondary antibodies (Novagen) were used for the detection of RibE.

Flavokinase assay and HPLC analysis of flavins. Flavokinase activity and quantitation of flavins was carried out as described (9). Specific flavokinase activity is expressed as nanomoles of phosphorylated flavin formed from the corresponding flavin and ATP per mg of protein. The values of K_m and V_{max} were deduced by fitting the initial reaction velocity to the

Michaelis-Menten equation based on a nonlinear regression using the software Sigma Plot (Systat, San Jose, CA, USA).

SI References

1. Mathes T, Vogl C, Stolz J, Hegemann P (2009) *In vivo* generation of flavoproteins with modified cofactors. *J Mol Biol* 385(5):1511-1518.
2. Saito H, Shibata T, Ando T (1979) Mapping of genes determining nonpermissiveness and host-specific restriction to bacteriophages in *Bacillus subtilis* Marburg. *Mol Gen Genet* 170(2):117-122.
3. Chan CM, Danchin A, Marliere P, Sekowska A (2014) Paralogous metabolism: S-alkyl-cysteine degradation in *Bacillus subtilis*. *Environ Microbiol* 16(1):101-117.
4. Sambrook J, Fritsch E, Maniatis T (1989) *Molecular cloning: a laboratory manual* (Cold Spring Harbor Laboratory, Cold Spring Harbor, NY) 2nd Ed.
5. Coppee JY, *et al.* (2001) Sulfur-limitation-regulated proteins in *Bacillus subtilis*: a two-dimensional gel electrophoresis study. *Microbiology* 147(Pt 6):1631-1640.
6. Defeu Soufo HJ, *et al.* (2010) Bacterial translation elongation factor EF-Tu interacts and colocalizes with actin-like MreB protein. *Proc Natl Acad Sci U S A* 107(7):3163-3168.
7. Pedrolli DB, *et al.* (2012) A highly specialized flavin mononucleotide riboswitch responds differently to similar ligands and confers roseoflavin resistance to *Streptomyces davawensis*. *Nucleic Acids Res* 40(17):8662-8673.
8. Fuhrer T, Heer D, Begemann B, Zamboni N (2011) High-throughput, accurate mass metabolome profiling of cellular extracts by flow injection-time-of-flight mass spectrometry. *Anal Chem* 83(18):7074-7080.
9. Mack M, van Loon AP, Hohmann HP (1998) Regulation of riboflavin biosynthesis in *Bacillus subtilis* is affected by the activity of the flavokinase/flavin adenine dinucleotide synthetase encoded by *ribC*. *J Bacteriol* 180(4):950-955.
10. Fischer M, Bacher A (2005) Biosynthesis of flavocoenzymes. *Nat Prod Rep* 22(3):324-350.
11. Jankowitsch F, *et al.* (2012) Genome sequence of the bacterium *Streptomyces davawensis* JCM 4913 and heterologous production of the unique antibiotic roseoflavin. *J Bacteriol* 194(24):6818-6827.
12. Skliarova SA, Kreneva RA, Perumov DA, Mironov AS (2012) [The characterization of internal promoters in the Bacillus subtilis riboflavin biosynthesis operon]. *Genetika* 48(10):1133-1141.
13. Vitreschak AG, Rodionov DA, Mironov AA, Gelfand MS (2002) Regulation of riboflavin biosynthesis and transport genes in bacteria by transcriptional and translational attenuation. *Nucleic Acids Res* 30(14):3141-3151.
14. Mehlhorn J, *et al.* (2013) A set of engineered Escherichia coli expression strains for selective isotope and reactivity labeling of amino acid side chains and flavin cofactors. *PLoS One* 8(11):e79006.
15. Pedrolli D, *et al.* (2015) The *ribB* FMN riboswitch from *Escherichia coli* operates at the transcriptional and translational level and regulates riboflavin biosynthesis. *Febs J.*
16. Mironov AS, *et al.* (2002) Sensing small molecules by nascent RNA: a mechanism to control transcription in bacteria. *Cell* 111(5):747-756.
17. Winkler WC, Cohen-Chalamish S, Breaker RR (2002) An mRNA structure that controls gene expression by binding FMN. *Proc Natl Acad Sci U S A* 99(25):15908-15913.

18. Ong LD, LeClare PC (1968) The Kolmogorov-Smirnov test for the log-normality of sample cumulative frequency distributions. *Health Phys* 14(4):376.
19. Kanehisa M, *et al.* (2014) Data, information, knowledge and principle: back to metabolism in KEGG. *Nucleic Acids Res* 42(Database issue):D199-205.
20. Macheroux P, Kappes B, Ealick SE (2011) Flavogenomics - a genomic and structural view of flavin-dependent proteins. *Febs J* 278(15):2625-2634.

Table S1 Kinetic constants for the flavokinase activities of RibR (and variants thereof) and RibFC from *Bacillus subtilis*

Protein	Specific activity (nmol mg^{-1} min^{-1})	K_M for riboflavin (μM)	k_{cat} (s^{-1})	k_{cat}/K_M (μM s^{-1})
MBP-RibR[a]	58 (±4)	11 (±1)	0.026	2.4 x 10^{-3}
MBP-RibR[b]	0.28 ± 0.2	nd[c]	nd	nd
MBP-N-RibR[d]	3.0	nd	nd	nd
MBP-C-RibR[e]	0	nd	nd	nd
MBP-RibFC	1,200 (±5)	55 (±2)	0.7	13 x 10^{-3}

[a]MBP-RibR (RibR amino acids 1-230)

[b]assayed in the presence of oxidized riboflavin

[c]nd = not determined

[d]MBP-N-RibR (RibR amino acids 1-89)

[e]MBP-C-RibR (RibR amino acids 90-230)

Table S2 Oligonucleotides used in this study

Number	Name	Sequence
1	ribRTAPfw	5‘-TCA TAG GTA CCC TCT AAC CTT GAA AAG ACA TTG GAG-3'
2	ribRTAPrev	5‘-TCA TGC TGC AGA CCT CCT CCC AAT ATA TTT TCT TC-3'
3	PribB.linker_fw	5‘-CAG CTG GCG TTG CTG CCG CTA ATC ATT AGC GTT ATA GTG AAT CCG CTT AAA GCT T-3‘
4	PribB.linker_rv	5‘-AAG CTT TAA GCG GAT TCA CTA TAA CGC TAA TGA TTA GCG GCA GCA ACG CCA GCT G-3‘
5	ribGRFN.HindIII_fw	5’-GAT AGT ACA AGC TTT AAG GAC AAA TGA ATA AAG ATT GTA TC-3'
6	ribGRFN.BamHI_rv	5’-CGC AGG ATC CCC AGC TTC ATA TAA TAC TCT TC-3'
7	ribURFN.HindIII_fw	5’-GAT AGT ACA AGC TTA ATT TCA TAT GAT CAA TCT TCG GGG CAG G-3'
8	ribURFN.BamHI_rw	5’-CGC AGG ATC CTG CTC AGC ATG CTG ACC ACA AC-3'
9	RFN(GGG18CCC)_fw	5'-GAA TAA AGA TTG TAT CCT TCC CCG CAG GGT GGA AAT CCC GAC CG-3'
10	RFN(GGG18CCC)_rv	5'-CGG TCG GGA TTT CCA CCC TGC GGG GAA GGA TAC AAT CTT TAT TC-3'
11	RFN(GGG23CCC)_fw	5'-GAT TGT ATC CTT CGG GGC ACC CTG GAA ATC CCG ACC GGC GG-3'
12	RFN(GGG23CCC)_rv	5'-CCG CCG GTC GGG ATT TCC AGG GTG CCC CGA AGG ATA CAA TC-3'
13	T7linker_fw	5’-AAT TCT AAT ACG ACT CAC TAT AGG GCC-3’
14	T7linker_rv	5’-CTC GAG GCC CTA TAG TGA GTC GTA TTA G-3’

15	ribDG-RFN.Apt_fw	5’-GAC TCT CGA GAG ATT GTA TCC TTC GGG GC-3’
16	ribDG-RFN.Apt_rv	5’-TAG CAA GCT TCA TCC TTC TCC CAT CC-3’
17	ribU-RFN.Apt_fw	5’-GAC TCT CGA GAT CAA TCT TCG GGG CAG-3’
18	ribU-RFN.Apt_rv	5’-TAG CAA GCT TAC CTC CAT CTT CTC CCA TCC-3’
19	RibR.NdeI_fw	5’-GCT ACA TAT GTT GAC GAT CAT TGC CGG TAC G-3’
20	RibR.XhoI_rv	5’-TCG ACT CGA GCT ATC CCA ATA TAT TTT CTT CAG-3’
21	RibR.Cterm.NdeI_fw	5’-GCT ACA TAT GAA AAT TAG AGA AAG GTT TG-3’
22	RibR.Nterm.XhoI_rv	5’-TCG ACT CGA GCT AAA TCC CAA TCA GCT CAA AGC G-3’
23	ribR-XbaI_fw	5‘-GAG GTC TAG AAT GAA AAT TAG AGA AAG G-3’
24	ribR-SmaI_rv	5‘-TGA CCC CGG GCT ATC CCA ATA TAT TTT CTT C-3’

SI Figure Legends

Fig. S1. The biosynthesis of riboflavin in *Bacillus subtilis* (10). All enzymatic steps (1.-9.) responsible for the conversion of GTP and two molecules of ribulose 5-phosphate into riboflavin, FMN and FAD are shown. Enzyme short names and EC numbers are shown above the arrows whereby abbreviations are according to the new genetic nomenclature proposed in an earlier work (11). RibAB is a bifunctional enzyme and is a GTP cyclohydrolase II (A) (EC 3.5.4.25) and a (3*S*)-3,4-dihydroxy-2-butanone 4-phosphate synthase (B) (EC 4.1.99.12). RibDG is a bifunctional 2,5-diamino-6-ribosylamino-4(3*H*)-pyrimidinone 5'-phosphate deaminase (D) (EC 3.5.4.26) and a 5-amino-6-ribosylamino-2,4(1*H*,3*H*)-pyrimidinedione 5'-phosphate reductase (G) (EC 1.1.1.193). RibH is a lumazine synthase (EC 2.5.1.78). RibE is a riboflavin synthase (EC 2.5.1.9). RibFC is a bifunctional flavokinase (F) (EC 2.7.1.26)/FAD synthetase (C) (EC 2.7.7.2). The phosphatase converting III to IV (step 4) is unknown. I, 2,5-Diamino-6-(5-phospho-D-ribosylamino)pyrimidin-4(3*H*)one; II, 5-Amino-6-ribosylamino-2,4(1*H*,3*H*)-pyrimidinedione 5'-phosphate; III, 5-Amino-6-ribitylamino-2,4(1*H*,3*H*)-pyrimidinedione 5'-phosphate; IV, 5-Amino-6-ribitylamino-2,4(1*H*,3*H*)-pyrimidinedione; V, (3*S*)-3,4-Dihydroxy-2-butanone 4-phosphate; VI, 6,7-Dimethyl-8-D-ribityllumazine. Notably, two molecules of VI dismutate (step 7) to give IV and riboflavin.

Figure S2. Genes responsible for riboflavin biosynthesis (A) and transport (B) in *Bacillus subtilis*. A. Schematic representation of the genes *ribDG-E-AB-H-T* (*rib* genes; yellow) responsible for riboflavin biosynthesis (*rib* operon). The transcription start site (TK start) downstream of the main σ70-dependent *rib*-promoter (ribGp1) is given in the box. Additional (minor) promoters (ribGp2 and ribGp3) were identified as shown (12). Expression of the *rib*-genes is controlled by the *ribDG* FMN riboswitch (triangle, transcriptional control) (13). Information with regard to the corresponding enzymes (RibDG, RibE, RibAB, RibH) can be found in Fig. S1. The function of *ribT* is yet unknown. The nucleotide positions refer to *B. subtilis* 168 (accession number AL009126.3). B. The gene *ribU* encodes a riboflavin

importer and its expression is controlled by the *ribU* FMN riboswitch (triangle, translational control) (13).

Figure S3. Methionine and taurine induce the synthesis of *Bacillus subtilis* RibR. SDS-SDS-PAGE/Western blot analysis of total soluble protein derived from cell-free extracts of a recombinant *B. subtilis* strain. In the analyzed strain RibR carried a tandem affinity purification-tag ("TAP-tag") which allowed monitoring of RibR synthesis employing anti-TAP-tag-antibodies. Cell-free extracts were prepared from cells grown in a minimal medium containing either methionine/taurine (RibR induction, lane 1) or $MgSO_4$ (RibR repression, lane 2). The same amount of total cellular protein was applied to each lane. Positions of molecular weight standards (in kDa) of a prestained protein marker (M) are shown. The upper band in lane 1 is RibR-TAP-tag (see bar), the lower band (with lower intensity) represents a degradation product. In the presence of $MgSO_4$ RibR-TAP-tag was not detected (lane 2).

Figure S4. Induction of RibR stimulates synthesis of *Bacillus subtilis* riboflavin synthase RibE. SDS-PAGE/Western blot analysis using anti-RibE antibodies of total soluble protein derived from cell-free extracts of *B. subtilis* wild-type. Cell-free extracts were prepared from cells grown in a minimal medium containing either $MgSO_4$ (RibR repression) (lane 1) or methionine/taurine (RibR induction) (lane 2). The same amount of total cellular protein was applied to each lane. Lane M shows the molecular weight standard (in kDa). The amount of RibE (monomer, 24 kDa) increased about 9-fold when RibR was induced by methionine/taurine (lane 2). The upper bands in lanes 1 and 2 represent dimers and tetramers of RibE. Lane 3 shows a purified RibE standard (monomeric form of RibE).

Figure S5. Scheme of coexpression experiments employing the specialized *Escherichia coli* strain CpXFMN. *E. coli* CpXFMN constitutively produces the riboflavin importer RibT from *Corynebacterium glutamicum* and thus (in contrast to a wild-type strain) is able to take up riboflavin (RF) added to the culture medium (14). Riboflavin is converted to the effector flavin mononucleotide (FMN) by *E. coli* flavokinase/FAD synthetase RibFC (15).

Transcriptional or translational fusion mRNAs of the two different *Bacillus subtilis* FMN riboswitches to *luc* are produced from the test plasmids pPrib-RibDG-RFN-luc or pPrib-RibU-RFN-luc (RFN = FMN riboswitch) (plasmid 1). In the presence of high levels of FMN the transcript adopts a structure terminating transcription (TK terminator) or preventing translation (TL sequestrator), luciferase is not produced (NO Luc signal). Low levels of FMN in turn lead to alternative structures of the FMN riboswitches, allowing *luc* expression (not shown). Coproduction of RibR (or variants thereof) is mediated by a second plasmid (plasmid 2) (pET28aribR) in the cytoplasm of *E. coli* CpXFMN. RibR overrides the FMN mediated "turn-off" activities of both *B. subtilis* FMN riboswitches and allows *luc* expression even in the presence of high levels of FMN.

Figure S6. Purification of *Bacillus subtilis* RibR from recombinant *Escherichia coli* strains. A. Polyacrylamide gel electrophoresis/Coomassie Brilliant Blue R-250 staining of protein samples collected from RibR-His_6 purification. M, molecular mass marker in kDa; Lane 1, purified His_6-tagged RibR (27 kDa) (denaturing conditions). Lane 2, purified His_6-tagged RibR (non-denaturing conditions). a, monomeric RibR-His_6; b, dimeric RibR-His_6; c, tetrameric RibR-His_6; d, octameric RibR-His_6. B. Polyacrylamide gel electrophoresis/Coomassie Brilliant Blue R-250 staining of protein samples collected from RibR-maltose binding protein (MBP) purification (MBP fusion proteins). M, molecular mass marker in kDa; Lane 1, MBP (43 kDa). Lane 2, MBP-RibR (MBP and full-length RibR, 70 kDa). Lane 3, MBP-RibR-C (MBP and C-terminal regulatory domain of RibR, 57 kDa). Lane 4, MBP-RibR-N (MBP and N-terminal flavokinase domain of RibR, 56 kDa).

Figure S7. $FMNH_2$ is a stronger effector of the *B. subtilis ribDG* FMN riboswitch when compared to FMN. The reporter plasmid pPrib-RibDG-RFN-luc generates a transcriptional fusion of the *ribDG* FMN riboswitch of *Bacillus subtilis* and the reporter gene *luc*. Expression from this plasmid is mediated by the *E. coli ribB* promoter sroGp2. pPrib-RibDG-RFN-luc was used as a template for an *in vitro* transcription/translation assay (driven by *Escherichia*

coli RNA polymerase) in the presence of different concentrations of flavin mononucleotide (FMN, solid spheres) and dihydroriboflavin mononucleotide ($FMNH_2$, open triangles), the reduced from of FMN. The addition of both flavins resulted in less Luc activity, indicating that less *luc* transcript was produced. This effect, however, was more pronounced in the presence of $FMNH_2$.

Figure S8. Sequence, proposed secondary structure i.e. expected transcriptional intermediates of variants of aptamer domains of the *Bacillus subtilis ribDG* FMN riboswitch in the presence of FMN (16, 17). A. The replacement of nucleotides G23, G24 and G25 by C23, C24 and C25 generated an FMN riboswitch variant which did not respond to the regulating activity of FMN anymore ("Mut ON") (16). B. The replacement of nucleotides G18, G19 and G20 by C18, C19 and C20 generated an FMN riboswitch which did not allow gene expression even in the absence of FMN ("Mut OFF") (16).

Figure S9. Global metabolic role of *ribR*. A wild-type *B. subtilis* strain and a *ribR* defective *B. subtilis* strain (*ribR::aph3*) were cultivated in six replicates to the exponential growth phase. Two different sulfur-sources were used during cultivation, $MgSO_4$ or a combination of methionine and taurine. Intracellular metabolites were extracted and analyzed employing nontargeted flow injection time-of-flight mass spectrometry (8). A. Number of ions with absolute fold-changes (*ribR::aph3* vs. wild type) of significantly affected metabolite ions (Student's $P < 0.05$) passing the indicated cutoffs. In the methionine/taurine medium more metabolite ions have higher fold-changes, consistent with *ribR* being expressed only in this condition. The difference of the two distributions was assessed by a Kolmogorov-Smirnov test (18). B. Volcano plot of detected metabolites involved in major sulfur assimilation pathways (KEGG pathway "sulfur metabolism"). C. Volcano plot of detected metabolites involved in riboflavin biosynthesis (see Fig. S1), according to the KEGG pathway definition (19). *P*-values were computed using Student's t-test. Selected metabolite ions (bold outline) are labeled by *m/z* and a possible annotation. D. Volcano plot of metabolite ions annotated as

substrates and products of flavoenzymes or other enzymes. For potential substrates or products of flavoenzymes, the EC number of the corresponding reaction is indicated. To identify which metabolites are processed by flavoenzymes, a list of potential flavoenzymes with fully characterized EC numbers (20) was matched with KEGG reactions occurring in *B. subtilis* to identify associated metabolites. A list of potential *B. subtilis* flavoenzymes and their substrates and products is included in Dataset S1.

Fig. S1.

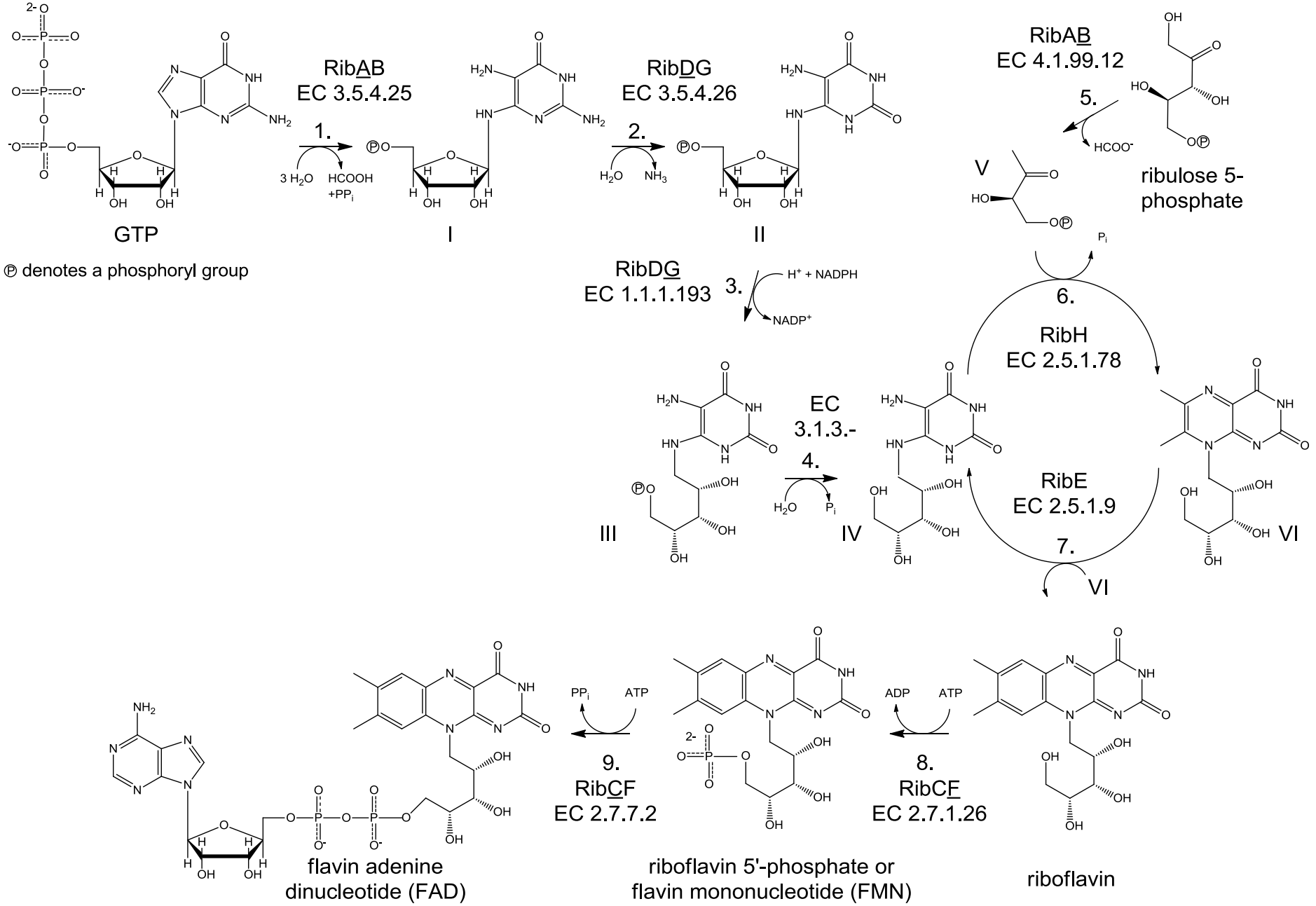
GTP
RibAB
EC 3.5.4.25
1.
3 H2O
HCOOH
+PPi
I
RibDG
EC 3.5.4.26
2.
H2O
NH3
II
Ⓟ denotes a phosphoryl group
RibAB
EC 4.1.99.12
5.
HCOO-
V
ribulose 5-
phosphate
RibDG
EC 1.1.1.193
3.
H+ + NADPH
NADP+
Pi
6.
RibH
EC 2.5.1.78
EC
3.1.3.-
4.
H2O
Pi
III
IV
RibE
EC 2.5.1.9
7.
VI
VI
flavin adenine
dinucleotide (FAD)
PPi
ATP
9.
RibCF
EC 2.7.7.2
riboflavin 5'-phosphate or
flavin mononucleotide (FMN)
ADP
ATP
8.
RibCF
EC 2.7.1.26
riboflavin

Fig. S2

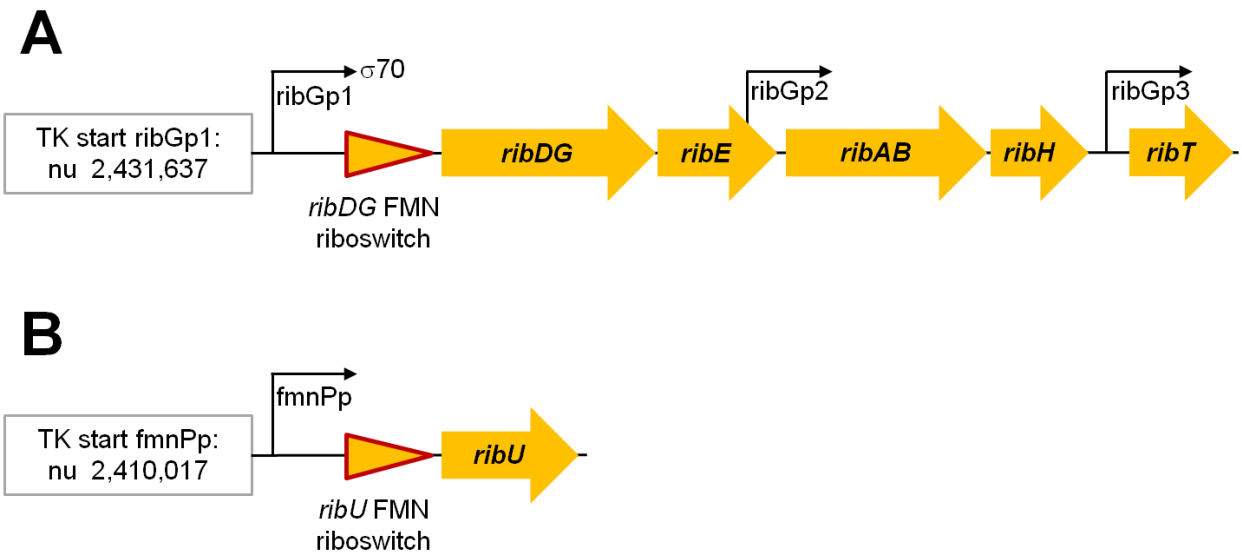
A
σ70
ribGp1
ribGp2
ribGp3
TK start ribGp1:
nu 2,431,637
ribDG
ribE
ribAB
ribH
ribT
ribDG FMN
riboswitch
B
fmnPp
TK start fmnPp:
nu 2,410,017
ribU
ribU FMN
riboswitch

Fig. S3

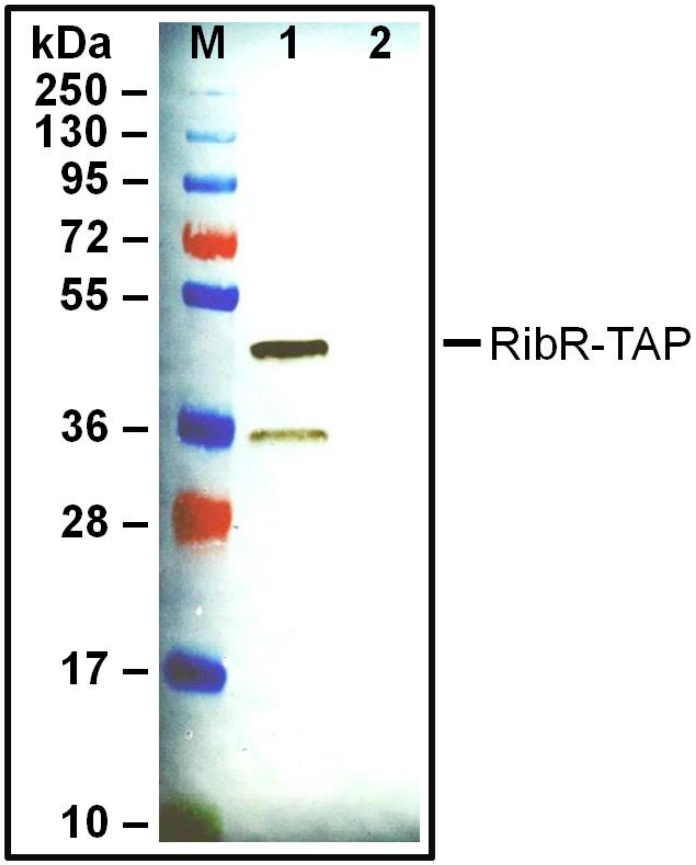

Fig. S4

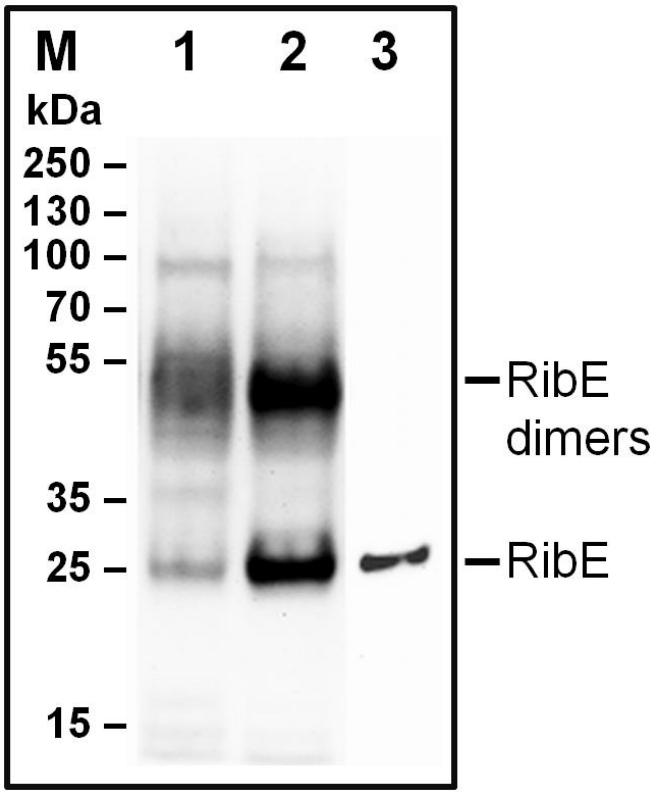

Fig. S5

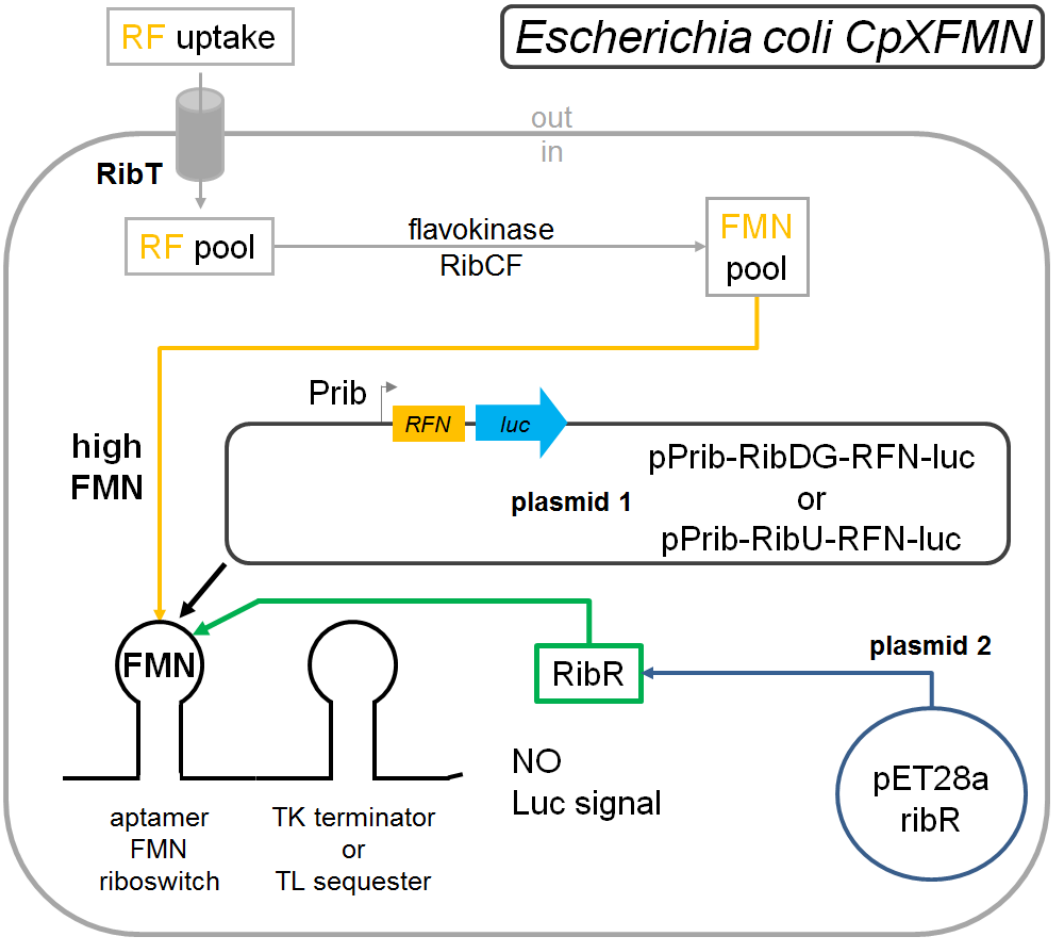
RF uptake
Escherichia coli CpXFMN
out
in
RibT
RF pool
flavokinase
RibCF
FMN
pool
Prib
RFN
luc
high
FMN
plasmid 1
pPrib-RibDG-RFN-luc
or
pPrib-RibU-RFN-luc
FMN
RibR
plasmid 2
NO
Luc signal
pET28a
ribR
aptamer
FMN
riboswitch
TK terminator
or
TL sequester

Fig. S6A

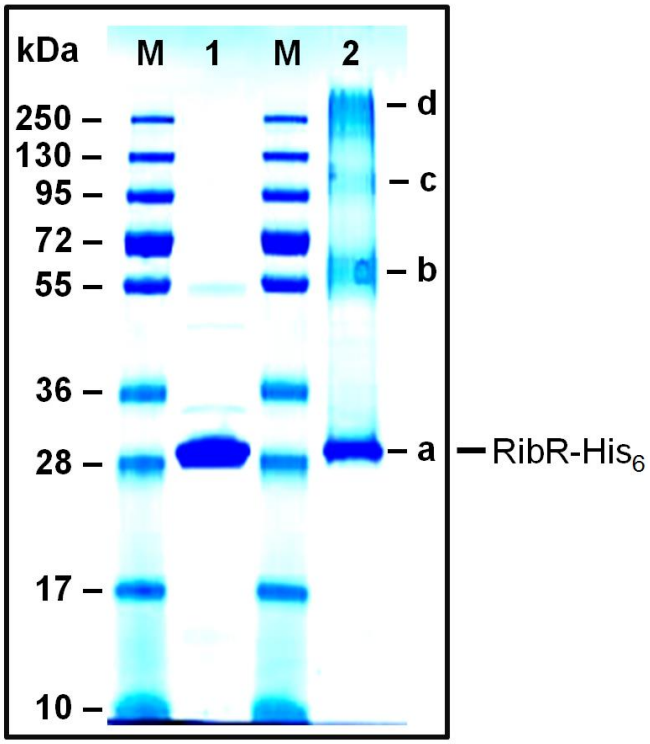

Fig. S6B

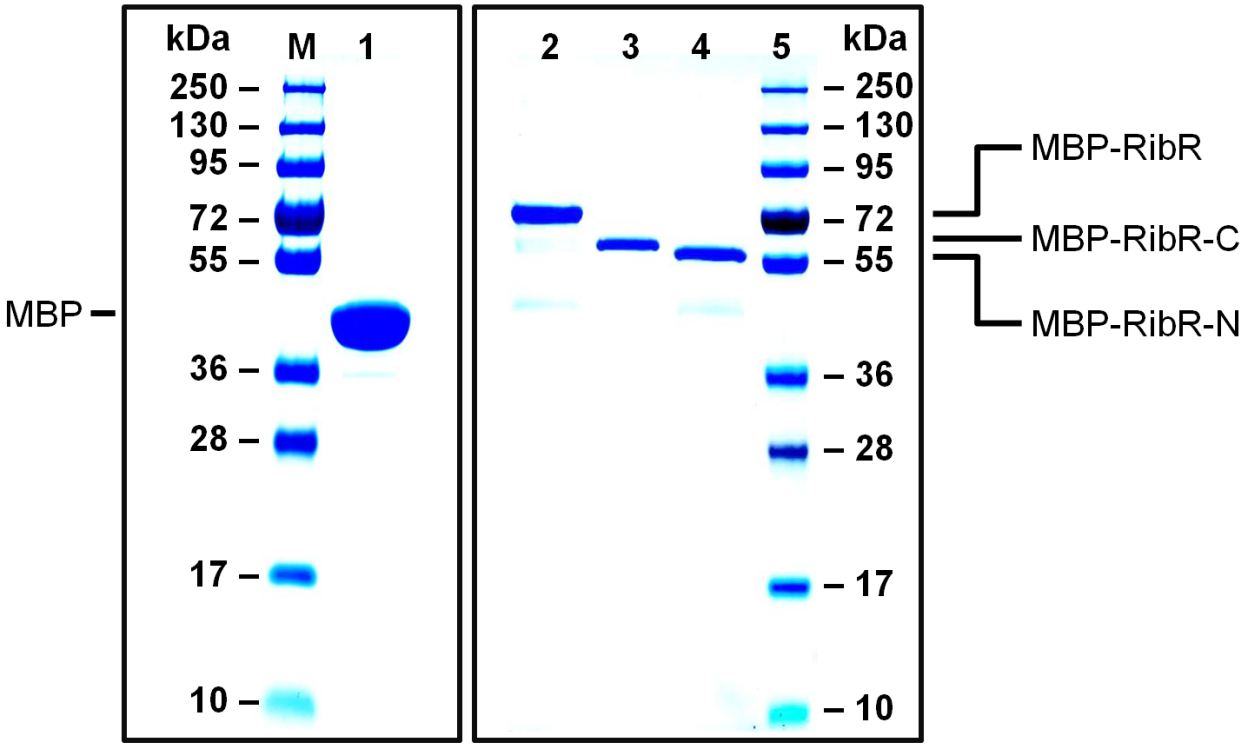

Fig. S7

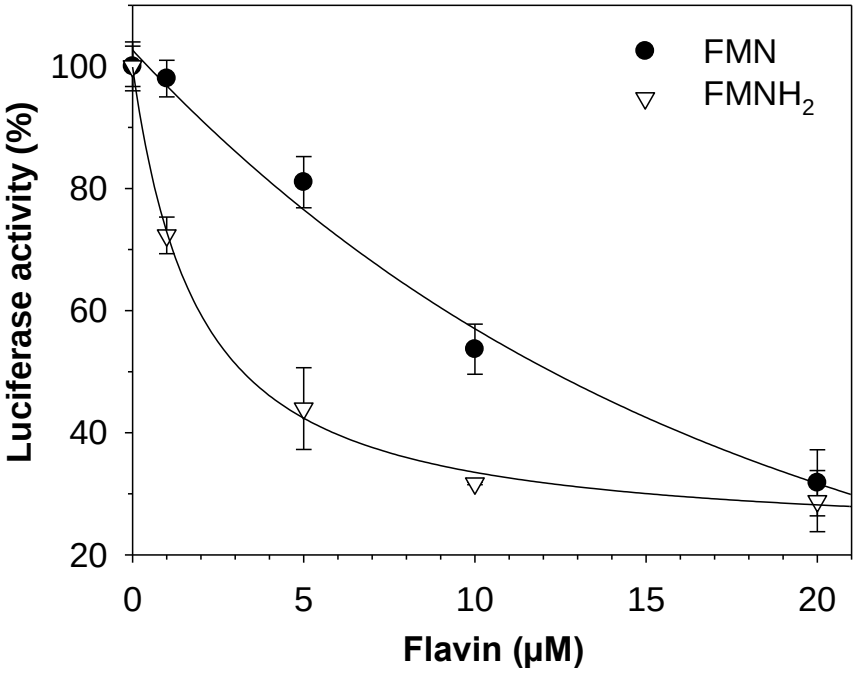
FMN
FMNH2
Luciferase activity (%)
100
80
60
40
20
0
5
10
15
20
Flavin (μM)

Fig S8A

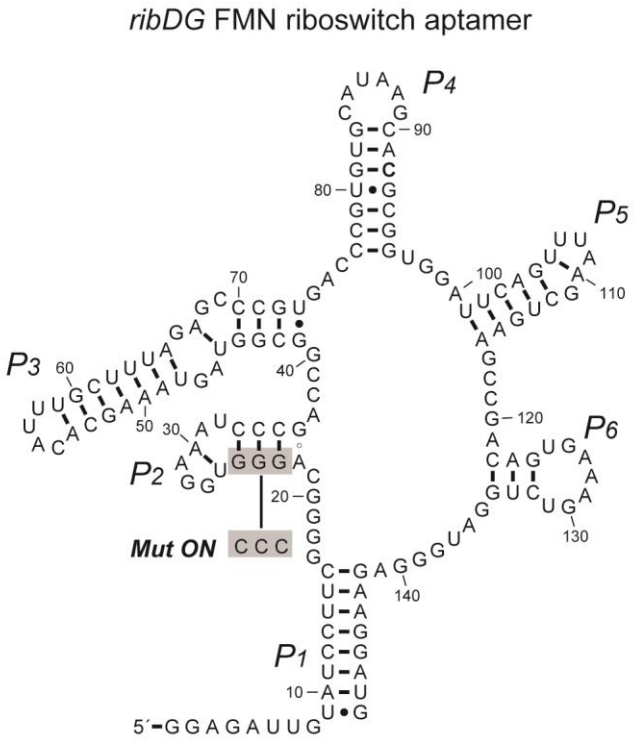

Fig S8B

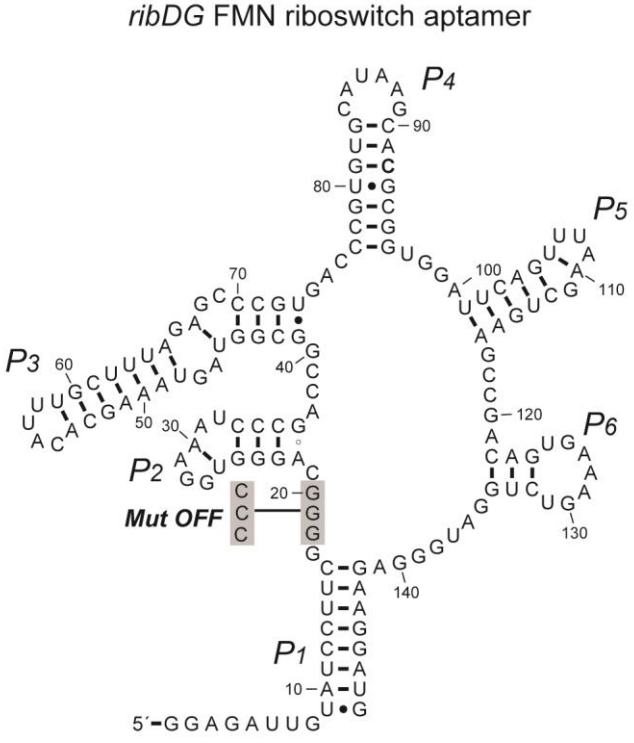

Fig. S9

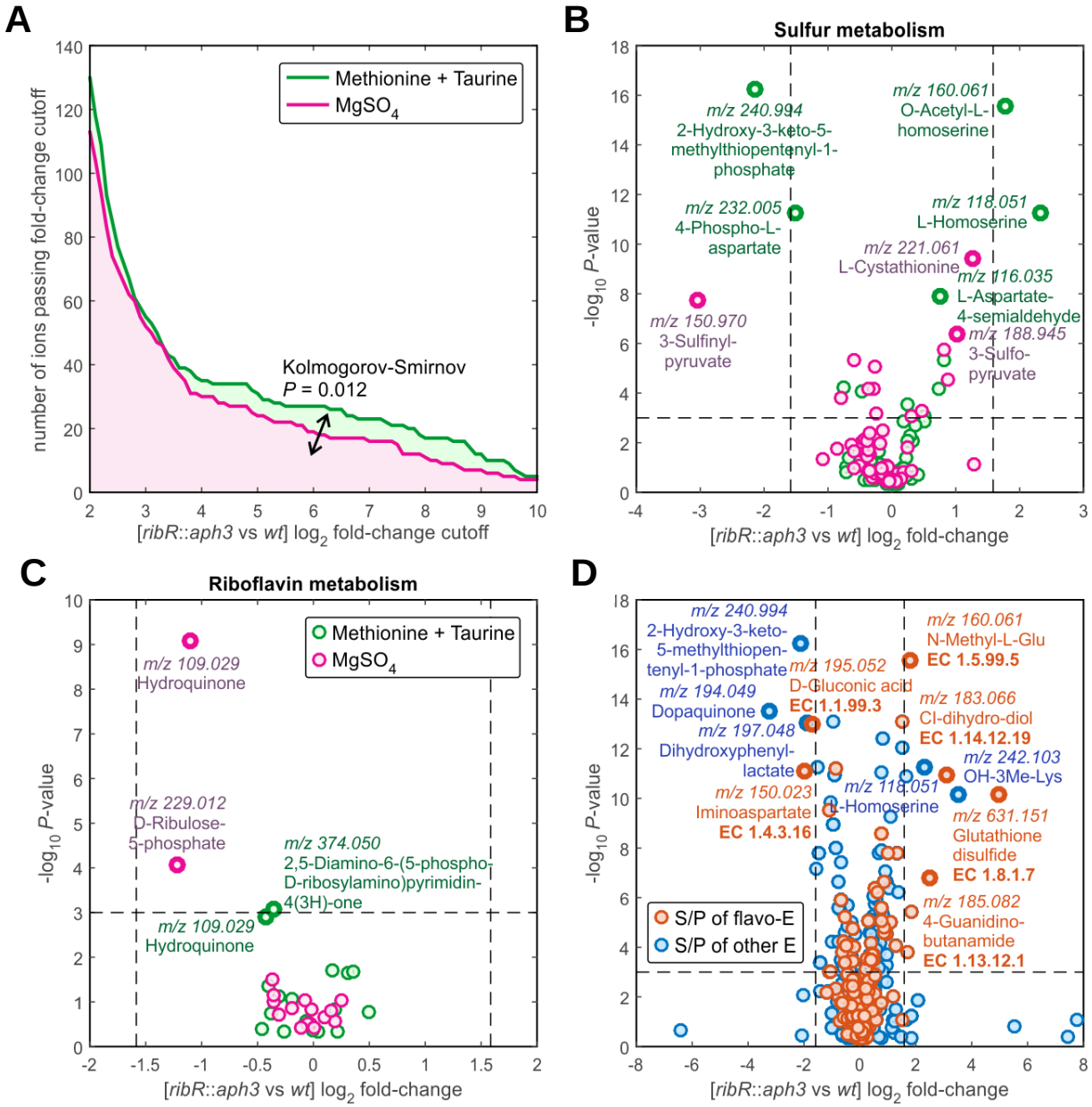
A
Methionine + Taurine
MgSO4
Kolmogorov-Smirnov
P = 0.012
number of ions passing fold-change cutoff
[ribR::aph3 vs wt] log2 fold-change cutoff
B
Sulfur metabolism
m/z 240.994
2-Hydroxy-3-keto-5-methylthiopentenyl-1-phosphate
m/z 160.061
O-Acetyl-L-homoserine
m/z 232.005
4-Phospho-L-aspartate
m/z 118.051
L-Homoserine
m/z 221.061
L-Cystathionine
m/z 116.035
L-Aspartate-4-semialdehyde
m/z 150.970
3-Sulfinyl-pyruvate
m/z 188.945
3-Sulfo-pyruvate
-log10 P-value
[ribR::aph3 vs wt] log2 fold-change
C
Riboflavin metabolism
Methionine + Taurine
MgSO4
m/z 109.029
Hydroquinone
m/z 229.012
D-Ribulose-5-phosphate
m/z 374.050
2,5-Diamino-6-(5-phospho-D-ribosylamino)pyrimidin-4(3H)-one
m/z 109.029
Hydroquinone
-log10 P-value
[ribR::aph3 vs wt] log2 fold-change
D
m/z 240.994
2-Hydroxy-3-keto-5-methylthiopentenyl-1-phosphate
m/z 160.061
N-Methyl-L-Glu
EC 1.5.99.5
m/z 195.052
D-Gluconic acid
EC 1.1.99.3
m/z 194.049
Dopaquinone
m/z 183.066
Cl-dihydro-diol
EC 1.14.12.19
m/z 197.048
Dihydroxyphenyl-lactate
m/z 242.103
OH-3Me-Lys
m/z 116.051
L-Homoserine
m/z 150.023
Iminoaspartate
EC 1.4.3.16
m/z 631.151
Glutathione disulfide
EC 1.8.1.7
m/z 185.082
4-Guanidino-butanamide
EC 1.13.12.1
S/P of flavo-E
S/P of other E
-log10 P-value
[ribR::aph3 vs wt] log2 fold-change